Differences in Intracardiac Signals on a Realistic Catheter Geometry using Mono- and Bidomain Models

Matthias W Keller, Steffen Schuler, Gunnar Seemann, Olaf Dössel

Institute of Biomedical Engineering, Karlsruhe Institute of Technology (KIT), Germany

Abstract

The correct interpretation of intracardiac electrograms is a key issue in the diagnosis and treatment of cardiac arrhythmias. Recent studies have suggested a link between local effects of substrate modification and the morphology of catheter signals. Studying these situations goes beyond the scope of most simulation studies as geometrical parameters and electrode conductivity are not taken into account. In this work a catheter model with realistic dimensions and conductivities is studied, comparing two approaches for the computation of extracellular potentials. One uses a monodomain simulation followed by a forward calculation of extracellular potentials. The other one is based on bidomain calculations that consider the influence of a metal electrode on the spread of depolarization. Calculated signals are compared to in-vivo signals reported in literature. Both approaches are capable of reproducing the morphology of clinical signals. Amplitudes are in the mV range and therefore in the right order of magnitude. Bidomain signals reproduce the time course more accurately, which could be related to wavefront curvature. Changes in transmembrane voltage were found due to the presence of the catheter in the bidomain case. Concluding from this study, for most cases the monodomain simulation seems to be sufficient, however for the investigation of small-scale changes bidomain simulations better represent in-vivo data.

1. Introduction

Catheter based measurements of intracardiac electrograms (IEGM) have become a standard technique in diagnosis and treatment of cardiac arrhythmias. A major technique to cure AF is the signal guided catheter ablation. The right interpretation of IEGMs and their underlying excitation patterns is a prerequisite for a successful treatment using this method. However for in-vivo measurements these patterns are hardly accessible. Therefore in-vitro and in-silico studies are powerful tools to address this issue. The linkage between certain excitation patterns occurring during atrial fibrillation and the corresponding catheter signals has been frequently studied. Simulation setups reached from 2D-patches [1], [2] to whole atria or whole heart simulations with forward calculated IEGMs [3]. The focus of these studies was the connection of excitation patterns during cardiac arrhythmias and their representation in extracellular signals. Therefore the geometry in most cases was reduced to virtual point electrodes. Simulations were performed by solving the monodomain equations and potentials were then forward calculated for extracellular space based on current source approximations [1], [2] or boundary element method [3]. Using these methods, interactions between extra- and intracellular space are not taken into account. Recently, the importance to interpret IEGMs in a more local way was pointed out for the evaluation of local activation mechanisms and scar transmurality [4], [5]. In this case a geometrically more detailed approach to study small-scale effects is necessary. In this work, EGMs were simulated on a realistic 3D catheter model. Different catheter orientations were taken into account. In this context full bidomain solutions were compared to the computational less expensive monodomain approach with subsequent forward calculations. Using the bidomain model, the influence of a highly conductive electrode on the spread of excitation can be investigated. Furthermore the wavefront curvature may alter the morphology of catheter signals. In general this study aims at a better understanding of the genesis of IEGMs in a 3D environment.

2. Methods

2.1. Simulation setups

Computational simulations of cardiac electrophysiology were performed in a 3D setup containing a rectangular shaped sheet of myocardium with a thickness of 4 mm, which has been reported for human atria [4]. Length (44.2 mm) and width (12 mm) were chosen to provide enough room to position the catheter and to avoid border effects in the catheter signals. Top and bottom layer of the myocardial sheet consist of a two voxel layer of passive endocardial tissue modeling the surface resistance of cardiac

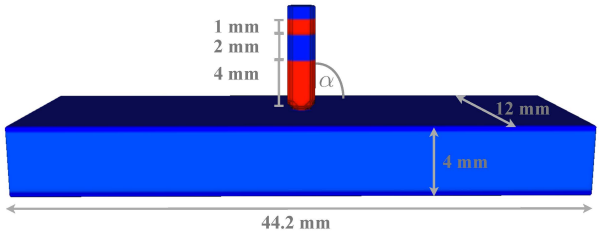

Figure 1. Tip of a 7F catheter with two electrodes (red), separated by insulation (blue), rectangular piece of myocardium (dark blue), setup filled with blood (not shown)

tissue. The catheter tip was modeled using the dimensions of a commonly used 4 mm-tip 7F ablation catheter with a second 1 mm electrode and an interelectrode spacing of 2 mm. The whole setup is surrounded by blood. The setup consists of cubical voxels with an edge length of 0.2 mm (see fig. 1). Five setups were created by varying catheter-tissue distance and catheter angle α for the investigation of different catheter positions (see fig. 2). Conductivity

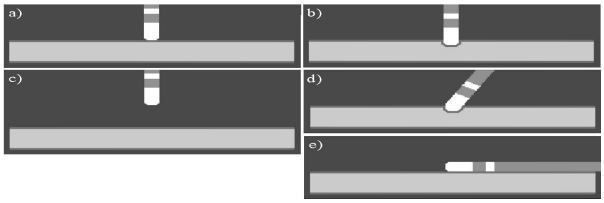

Figure 2. Simulation setups: a) S1: touching, b) S2: indented, c) S3: not touching, d) S4: angled at 60°, e) S5: parallel

values were chosen as listed in table 1. All conductivities are isotropic to allow comparison between different setups. Intracellular conductivities for myocardium were chosen to match a conduction velocity of 700 mm/s, which is a medium value reported for atrial human tissue [6]. Extracellular values for myocardium were set to values reported in literature [7]. Real metal conductivity of 10^6 S/m led to numerical instabilities in preliminary studies. Therefore, it was set 1000 times higher than the conductivity of blood. Using this value the electrode still formed an equipotential surface. The Courtemanche et al. model [8] was used,

Table 1. Conductivities in simulation setups (S/m)

Material	σ_M	σ_i	σ_e
Myocardium	0.245	0.5	0.2
Endocardium	10^{-10}	10^{-10}	0.1
Blood	10^{-10}	10^{-10}	0.7
Catheter electrodes	10^{-10}	10^{-10}	700
Insulation	10^{-22}	10^{-22}	10^{-22}

which represents a human atrial cell.

2.2. Calculation of extracellular potential and catheter signals

From bidomain simulations, extracellular potential ϕ_e was received directly for all points in the simulated volume. In the monodomain case, a two-step process was performed. In a first step, the monodomain equation as shown in equation 1 was solved,

$$\nabla \cdot (\sigma_M \nabla V_m) = \beta(C_m \frac{dV_m}{dt} + I_{mem}) = \beta I_m \quad (1)$$

with the monodomain conductivity σ_M, the transmembrane voltage V_m and cell-surface to volume ratio β. Calculated transmembrane currents I_m were then used as input for equation 2 which is derived from the second bidomain equation.

$$-\nabla \cdot (\sigma_e \nabla \phi_e) = \beta I_m \quad (2)$$

Based on the extracellular potentials on the distal electrode $\phi_{e,d}(t)$ and proximal electrode $\phi_{e,p}(t)$ catheter signals were calculated. Bipolar EGMs $V_{bip}(t)$ are the difference of $\phi_{e,p}(t)$ and $\phi_{e,d}(t)$. For unipolar EGMs $V_{uni}(t)$ the mean of the extracellular potentials in the total volume $\phi_{e,mean}(t)$ served as a stable reference potential.

2.3. Evaluation of simulation results

One major difference between the two simulation approaches is the feedback between intra- and extracellular space. In order to quantify the influence of a touching catheter on V_m, two bidomain simulations were performed: One setup with a catheter touching the tissue and one without catheter. The difference in V_m between the two simulations for each time step illustrates changes in V_m caused by catheter-tissue interactions. Signals of setups 1-3 were compared in order to study signal changes due to electrode tissue distance. For a comparison of EGM amplitudes, signals from both approaches were normalized to have an intramural unipolar signal amplitude of 20 mV underneath the catheter tip, which was reported from plunge electrode recordings [9]. Along with the intramural EGMs all other signals were multiplied with the extracted scaling factor.

2.4. Comparison to in-vivo signals

Characteristic signal parameters from Otomo et al. [4], who performed catheter measurements in pig atria were used to evaluate the signal morphology. Specifically, the peak to peak amplitude of uni- and bipolar signals (A_{pp}) as well as the EGM width for bipolar signals (ΔW) was

compared. For simulated signals ΔW were calculated between the onset and end of the EGM defined as the points in time where the signal amplitude rose above respectively fell below 1% of the maximum deflection amplitude.

3. Results

3.1. Transmembrane voltage

The characteristic wavefront curvature of V_m resulting from bidomain simulations can be seen in figure 3, a). In a monodomain simulation however the wavefront is planar as no interference between intra- and extracellular space occurs. The plot 3, b) shows the difference in transmembrane potential ΔV_m calculated from V_m of two simulations, one with catheter, one without. Underneath the catheter a difference of 5 mV is present.

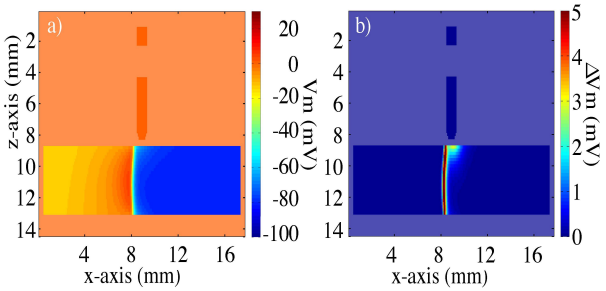

Figure 3. a) V_m as a result of a bidomain simulation. b) ΔV_m between two simulations with and without catheter

3.2. Simulated catheter signals

The resulting catheter signals from amplitude comparison are depicted in figure 4. Absolute values for amplitudes are given in table 2. Unipolar EGMs show a positive

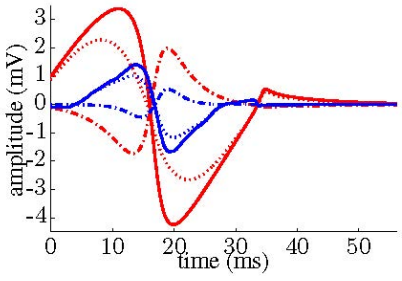

Figure 4. Signals from setup 1: bido (red), mono (blue), dist. unip. (straight), prox. unip. (dotted), bip. (dashed)

to negative deflection. For bipolar EGMs the polarity is inverted. Amplitudes roughly differ by a factor of two for unipolar and by a factor of four for bipolar EGMs. Comparison of signals from setups 1-3 shows good agreement

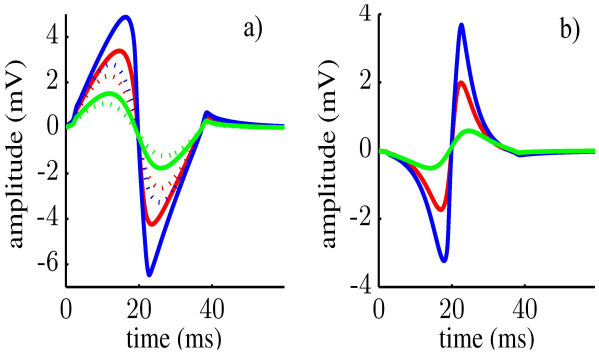

Figure 5. Bidomain signals, setups 1-3 (red,blue,green); a) unip. dist. (straight), prox. (dotted); b) bipolar

with clinical data. Amplitude and peakedness increase with decreasing distance between electrode and tissue (see fig. 5).

3.3. Comparison to in-vivo signals

Characteristic signal values for parallel and non-parallel catheter orientations as reported in-vivo [4] were derived from the simulations (see tables 2, 3). For setup 1 the amplitude of unipolar EGMs calculated by the monodomain approach is roughly the same or below the measured amplitudes whereas bidomain amplitudes are by a factor of two higher. Also, for the bipolar EGMs, the simulations

Table 2. Non-parallel orientation, A_{pp} (mV), ΔW (ms)

Setup 1	A_{pp}, V_{bip}	A_{pp}, V_{dist}	A_{pp}, V_{prox}	ΔW
Bido	3.72	7.63	4.94	35.7
Mono	0.99	3.08	2.19	27.0
In-vivo	2.00	3.20	1.10	40.0

deviated by a factor of two. The window size (ΔW) is better matched by the bidomain solution. Regarding the

Table 3. Parallel orientation, A_{pp} (mV), ΔW (ms)

Setup 5	A_{pp}, V_{bip}	A_{pp}, V_{dist}	A_{pp}, V_{prox}	ΔW
Bido	9.54	8.79	8.76	22.0
Mono	2.94	3.17	3.74	16.4
In-vivo	3.80	3.20	3.10	30.0

parallel catheter orientation of setup 5, again the amplitude deviations are smaller for the monodomain approach. The window size, however, is less accurately represented by this signal. A set of EGMs was extracted from Otomo's data (see fig. 6a) in order to illustrate the temporal course

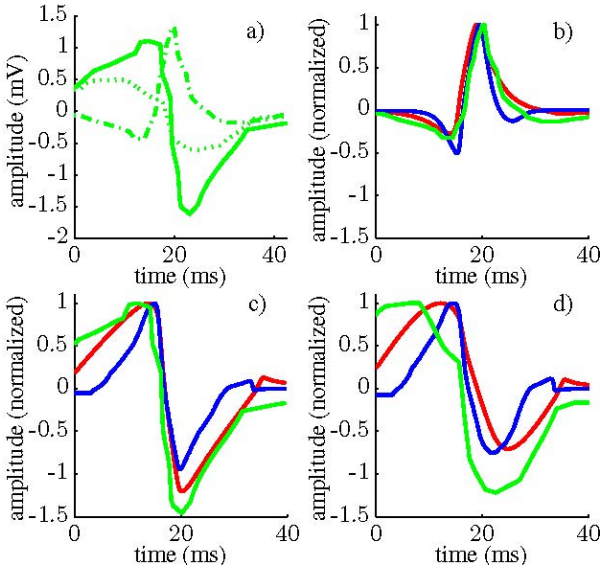

Figure 6. Comparison of setup 4 to in-vivo data; a) in-vivo signals [4]: dist. (straight), prox. (dotted), bip. (dashed); b) bip.; c) unip. distal; d) unip. proximal; red: bido, blue: mono, green: in-vivo

of the catheter signals. Figures 6 b-d show the three leads of setup 4 (60 ° angle) superimposed on the leads of the extracted data. For better comparison each group was scaled to the same maximum amplitude and shifted in time to the point of greatest deflection.

4. Discussion and conclusion

Simulated signal morphology showed a positive to negative deflection for unipolar- and a negative to positive deflection for bipolar signals, which is in agreement with in-vivo data. Time course and morphology were reproduced correctly by simulated signals of both approaches. Especially, the temporal course for non-parallel catheter orientation closely matched measured data. Amplitudes were in the right order of magnitude but deviated up to a factor of three from in-vivo values, which could be explained by electrode impedance in real measurements. Signals showed an expected change in EGM amplitude and peakedness with varying distance between catheter and tissue. In bidomain simulations a curved wavefront in transmural spread of excitation and a change in V_m due to the electric load of the catheter was identified. Overall both approaches were able to reproduce the coarse morphology of IEGMs. Going more into detail, the window width ΔW was better represented by bidomain signals which can be explained by wavefront curvature which leads to a broader EGM and therefore a better representation in time. Additionally, interactions between catheter load and cardiac electrophysiology can be investigated using the bidomain approach. Based on this study further investigations regarding IEGM genesis and interpretation are possible and may lead to new insights how tissue alterations, e.g. ablation scars, in the vicinity of the catheter tip can lead to changes in catheter signals.

Acknowledgements

The work of Matthias Keller is funded by the German Research Foundation (DFG)

References

[1] Jacquemet V, Henriquez CS. Genesis of complex fractionated atrial electrograms in zones of slow conduction: a computer model of microfibrosis. Heart Rhythm Jun 2009; 6(6):803–10.

[2] Richter U, Faes L, Cristoforetti A, Masè M, Ravelli F, Stridh M, Sörnmo L. A novel approach to propagation pattern analysis in intracardiac atrial fibrillation signals. Ann Biomed Eng Jan 2011;39(1):310–23.

[3] Zhu X, Wei D. Computer simulation of intracardiac potential with whole-heart model. Int J Bioinform Res Appl 2007; 3(1):100–22.

[4] Otomo K, Uno K, Fujiwara H, Isobe M, Iesaka Y. Local unipolar and bipolar electrogram criteria for evaluating the transmurality of atrial ablation lesions at different catheter orientations relative to the endocardial surface. Heart Rhythm Sep 2010;7(9):1291–300.

[5] Tedrow UB, Stevenson WG. Recording and interpreting unipolar electrograms to guide catheter ablation. Heart Rhythm May 2011;8(5):791–6.

[6] Weber FM, Schilling C, Seemann G, Luik A, Schmitt C, Lorenz C, Dössel O. Wave-direction and conduction-velocity analysis from intracardiac electrograms–a single-shot technique. IEEE Transactions on Biomedical Engineering 2010; 57:2394–2401.

[7] Colli Franzone P, Guerri L, Taccardi B. Potential distributions generated by point stimulation in a myocardial volume: simulation studies in a model of anisotropic ventricular muscle. Journal of Cardiovascular Electrophysiology 1993; 4:438–458.

[8] Courtemanche M, Ramirez RJ, Nattel S. Ionic mechanisms underlying human atrial action potential properties: Insights from a mathematical model. Am J Physiol 1998;275:H301–H321.

[9] Rogers J, Melnick S, Huang J. Fiberglass needle electrodes for transmural cardiac mapping. Biomedical Engineering IEEE Transactions on dec. 2002;49(12):1639 –1641. ISSN 0018-9294.

Address for correspondence:

Matthias Keller, KIT - Institute of Biomedical Engineering, Fritz-Haber-Weg 1, 76131 Karlsruhe, Germany
publications@ibt.kit.edu